Atmos. Meas. Tech., 17, 5887–5901, 2024
https://doi.org/10.5194/amt-17-5887-2024

Atmospheric Measurement Techniques
Open Access
EGU

Evaluation of a reduced-pressure chemical ion reactor utilizing adduct ionization for the detection of gaseous organic and inorganic species

Matthieu Riva[1,2,★], Veronika Pospisilova[1,★], Carla Frege[1], Sebastien Perrier[2], Priyanka Bansal[1], Spiro Jorga[1], Patrick Sturm[1], Joel A. Thornton[3], Urs Rohner[1], and Felipe Lopez-Hilfiker[1]

[1]TOFWERK, 3645 Thun, Switzerland
[2]Université Claude Bernard Lyon 1, CNRS, IRCELYON 69626, Villeurbanne, France
[3]Department of Atmospheric Sciences, University of Washington, Seattle, WA 98195, USA
★These authors contributed equally to this work.

Correspondence: Matthieu Riva (matthieu.riva@tofwerk.com) and Felipe Lopez-Hilfiker (lopez@tofwerk.com)

Received: 28 March 2024 – Discussion started: 19 April 2024
Revised: 13 July 2024 – Accepted: 18 July 2024 – Published: 7 October 2024

Abstract. Volatile organic compounds (VOCs) and volatile inorganic compounds (VICs) provide critical information across many scientific fields including atmospheric chemistry and soil and biological processes. Chemical ionization (CI) mass spectrometry has become a powerful tool for tracking these chemically complex and temporally variable compounds in a variety of laboratory and field environments. It is particularly powerful with time-of-flight mass spectrometers, which can measure hundreds of compounds in a fraction of a second and have enabled entirely new branches of VOC and/or VIC research in atmospheric and biological chemistry. To accurately describe each step of these chemical, physical, and biological processes, measurements across the entire range of gaseous products is crucial. Recently, chemically comprehensive gas-phase measurements have been performed using many CI mass spectrometers deployed in parallel, each utilizing a different ionization method to cover a broad range of compounds. Here we introduce the recently developed Vocus AIM (adduct ionization mechanism) ion–molecule reactor (IMR), which samples trace vapors in air and ionizes them via chemical ionization at medium pressures. The Vocus AIM supports the use of many different reagent ions of positive and negative polarity and is largely independent of changes in the sample humidity. Within the present study, we present the performance and explore the capabilities of the Vocus AIM using various chemical ionization schemes, including chloride (Cl^-), bromide (Br^-), iodide (I^-), nitrate (NO_3^-), benzene cations ($C_6H_6^+$), acetone dimers ($(C_3H_6O)_2H^+$), and ammonium (NH_4^+) reagent ions, primarily in laboratory and flow tube experiments. We report the technical characteristics and operational principles, and compare its performance in terms of time response, humidity dependence, and sensitivity to that of previous chemical ionization approaches. This work demonstrates the benefits of the Vocus AIM reactor, which provides a versatile platform to characterize VOCs and VICs in real time at trace concentrations.

1 Introduction

Mass spectrometry represents a nearly universal method for determining the chemical composition of organic and inorganic species across various environmental matrices. In the fields of environmental and atmospheric chemistry, chemical ionization (CI) is a versatile real-time method to measure individual organic and inorganic compounds in air at trace concentrations (Yuan et al., 2017; Riva et al., 2019; W. Zhang et al., 2023; Y. Zhang et al., 2023). As in all chemical ionization systems, trace analytes in air react with excess reagent ions, leading to the formation of charged product ions usually via electron/proton transfer or adduct formation (W. Zhang et al., 2023; Y. Zhang et al., 2023). Advances in the field of chemical ionization over the last decade have yielded excep-

tionally low detection limits down to 10^4 molec. cm^{-3} (parts per quadrillion), expanded dynamic ranges, and the capability of measuring a wide range of gaseous organic and inorganic species with time resolutions of up to 50 Hz (Riva et al., 2019; W. Zhang et al., 2023; Y. Zhang et al., 2023).

Chemical ionization mass spectrometers are uniquely able to measure temporal variability in trace volatile organic compound (VOC) and atmospheric oxidation products in both the laboratory and the field, providing a critical tool to mechanistically track the most important atmospheric oxidation processes (Hallquist et al., 2009; Ehn et al., 2014; Bianchi et al., 2019). In particular, CI has made enormous improvements in the detection and quantification of reactive gaseous oxygenated species, including peroxy (RO_2) radicals, stabilized Criegee intermediates, and inorganic acids and bases that are difficult to directly detect with any other available analytical technique (Berndt et al., 2015, 2017, 2018; Breitenlechner et al., 2017; Hansel et al., 2018; Krechmer et al., 2018). For example, measurements via chemical ionization mass spectrometry (CIMS) have been pivotal in discovering the existence and importance of extremely low volatility organic molecules (ELVOCs). These compounds are now understood to be formed ubiquitously in the atmosphere and are critical to new particle formation and growth (Ehn et al., 2014; Bianchi et al., 2019). As a result, CIMS has emerged as a core analytical tool in atmospheric chemistry and related fields that require high sensitivity, high temporal resolution, and molecular-level speciation (Bruderer et al., 2019; Riva et al., 2019; Tang et al., 2019; Mazzucotelli et al., 2022; W. Zhang et al., 2023; Y. Zhang et al., 2023).

With the right selection of reagent ions, CI offers the possibility of soft, selective, and sensitive online detection for essentially any class of chemical compounds. While in practice, no reagent ion can simultaneously detect the entire distribution of volatile compounds present in the atmosphere with sufficient selectivity and sensitivity, different reagent ions can be selected to target distinct chemical families (Crounse et al., 2006; Bertram et al., 2011; Kim et al., 2016; Lee et al., 2014; Bianchi et al., 2019; Riva et al., 2019; W. Zhang et al., 2023; Y. Zhang et al., 2023). Therefore, a critical choice for chemical ionization operators is which reagent ion is best suited to measure compounds of interest in each measurement scenario.

Recent advancements in the design of the reactor have sought to improve measurement quality by addressing two outstanding limitations of chemical ionization mass spectrometers: (i) improved detection efficiency by refining the reactor geometry and optimizing the flow dynamics within the system and (ii) reliable, reproducible, and fully controlled reaction conditions. Improvements in the detection efficiency depend on the balance of two critical parameters in any chemical ionization reactor. First, compounds present in the sample gas stream need to be efficiently transported to the reaction cell and to mix/react with the reagent ions. The efficiency of the first step depends primarily on ionization pressure and absolute flow rate (i.e., residence time). At atmospheric pressure, gases diffuse slowly, and maintaining laminar flows between the sample line and reaction cell is straightforward (e.g., Eisele-inlet, MION, Crossflow CIMS) (Eisele and Tanner, 1993; Palm et al., 2019; Rissanen et al., 2019; Pfeifer et al., 2020). However, operating at high pressure makes controlling ionization conditions much more challenging. Therefore, most CIMS instruments operate at a reduced pressure to facilitate control of the ionization conditions. Sample vapors enter most reduced-pressure chemical ionization mass spectrometers through a critical orifice, which introduces turbulence as the gas expands into the reaction cell. This turbulence can introduce contact between the neutral sample gas and the reactor walls, resulting in memory effects and losses of reactive trace compounds by collision with the walls. While there have been numerous efforts to improve the introduction of sample gases into reduced-pressure reactors by laminarizing (Palm et al., 2019) the incoming airflow or by controlling the expansion inside of specially coated glass tubes (Vasquez et al., 2018), these approaches are often complex and demand considerable optimization, which has hindered their widespread adoption. Consequently, turbulent wall losses and memory effects continue to pose substantial challenges in reduced-pressure chemical ionization instruments, particularly when detecting reactive or sticky compounds.

Operating chemical ionization instruments at reduced pressure provides more refined control over ion chemistry since it allows for more straightforward and effective manipulation of ions within the instrument. Of particular nuisance in nearly all chemical ionization approaches is water vapor, which is highly variable and can have significant effects on the chemical ionization process. The formation of water clusters, which grow rapidly as a function of increasing pressure, presents a specific challenge for measurements taken near atmospheric pressure. Even chemical ionization approaches that operate at low pressures, such as proton transfer reaction (PTR), can be affected by the presence of water vapor (Yuan et al., 2017). PTR instruments are widely used for the detection of trace VOCs using high electric fields to control the reagent ion populations under changing humidity. While PTR instruments can largely control the ionization and collision conditions in the reactor, applying high electric fields results in extensive fragmentation of some critical functional groups in many fields (Yuan et al., 2017). Further, the PTR ionization process is well known to lead to significant fragmentation of labile compounds such as acids, peroxides, and alcohols. The fragmentation induced by protonation or charge transfer reactions along with elevated collision energy within the reactor significantly complicate the mass spectrum, in some cases limiting the possibility of retrieving the accurate concentration and composition of many classes of compounds including highly oxygenated and functionalized organic species.

To improve the sensitivity (specificity) and reduce the degree of fragmentation, softer chemical ionization techniques relying on adduct formation have become increasingly popular, especially when molecular identification and mechanistic pathways must be accurately tracked. These reactors operate under low ($E/N < 10$ Td) or field-free conditions at pressures typically from 50 to 500 mbar to promote adduct formation and stabilization (W. Zhang et al., 2023; Y. Zhang et al., 2023). Fluid dynamics and the degree of turbulence inside the reactor govern reaction times and ion transport in such reactors. At these elevated ionization pressures, the effect of water vapor can become a critical parameter affecting sensitivity. Routinely used reagent ions can result in order-of-magnitude changes in sensitivity under atmospherically relevant fluctuations in humidity (Lee et al., 2014; Breitenlechner et al., 2017; W. Zhang et al., 2023; Y. Zhang et al., 2023). Correcting the data for each compound's humidity dependence is an error-prone and time-consuming process where each compound must be treated essentially individually. Flooding the reactor with water vapor as is done in techniques like Vocus PTR can suppress the humidity dependence of some compounds. Such approaches are only applicable to certain groups of compounds whose water vapor dependence becomes weaker at higher absolute concentrations of water, which is not a universal characteristic. In general, the lack of adequate water vapor control remains a major drawback of chemical ionization systems, most critically those operated at pressures greater than 10 mbar.

Herein we introduce the Vocus AIM (adduct ionization mechanism) ion molecule reactor (IMR) and report the technical characteristics, operation principle, and performance of this new chemical reactor. We evaluate its performance by reporting the time response of nitric acid, demonstrate a novel approach to suppress humidity dependence, and compare sensitivity to other CI reactors. We present the design and capabilities of the Vocus AIM using a wide variety of reagent ions, including chloride (Cl^-), bromide (Br^-), iodide (I^-), nitrate (NO_3^-), benzene cations ($C_6H_6^+$), acetone dimers ($(C_2H_5O)_2H^+$), and ammonium (NH_4^+) ions. Finally, we show the measurement of RO_2 radicals and oxygenated VOCs acquired during the proof-of-concept experiment of OH/O_3-initiated oxidation of α-pinene. This work highlights the benefits of the Vocus AIM reactor within atmospheric chemistry and shows its limitations.

2 Experimental section

2.1 Vocus AIM reactor design

Medium-pressure chemical ionization (20–500 mbar) systems are typically designed as flow tube reactors that primarily transport ions toward the reactor exit by gas flow. Manipulating ions at high pressure would require high electric fields, which are impractical or could fragment the labile analyte ions. Further, RF devices that could focus ions into a beam do not efficiently operate at such high pressures, precluding their efficient use. Therefore, the Vocus AIM reactor operates on many of the same fundamental principles of more traditional flow tube reactors, including field-free ionization conditions (Fig. 1) and fluid dynamic transport of ions through the reactor. Specifically, the new design includes improvements in sample and reagent ion introduction, a conductive polytetrafluoroethylene (cPTFE) Teflon® conical reaction chamber to improve time response, and a simple yet efficient quadrupole-based differentially pumped time-of-flight (TOF) interface.

Gases enter the reactor manifold via a 1/2 in. o.d. Swagelok fitting, which is pumped through an inlet via a radially symmetric pump port. Excess flow is used to maintain short residence time and to minimize inlet memory effects such as surface reaction (conversion) and irreversible wall losses. Typical make-up flow rates of 5–10 slpm (standard liters per minute) are used to transport neutral analytes efficiently to the entrance of the reactor. A bored-through Swagelok interface ensures that all wetted surfaces before the reactor are Teflon®, to minimize the retention and memory of the inlet line for semi-volatile gases and reduce surface activity. At the entrance of the Vocus AIM IMR, the sample flow enters directly into the center of the conical reactor at a flow rate of 1.8 slpm through a stainless-steel critical orifice (0.475 mm) and a PFA Teflon® sample flow guide, which promotes subsampling from the center of the laminar inlet flow. The reactor is typically operated at a pressure of 50 mbar as a compromise between sensitivity and linear range and is controlled by a pressure control valve and an IDP3 vacuum pump (Agilent Technologies, IDP3). The reactor is temperature controlled to 50 °C, which is the lowest temperature that can be reliably controlled across various field conditions, to ensure constant reaction conditions. While a lower reactor temperature would promote adduct formation, the long-term stability of thermal conditions would be more difficult to maintain. Reagent ions are generated by compact vacuum ultraviolet (VUV) ion sources arranged radially around the central axis, with reactant ions injected at an angle (45°) to intersect the expanding sample flow with minimal sample deflection and ensure that no VUV light directly enters the IMR. Each ion source introduces the ions into the reactor with a standard flow rate of 0.25 slpm for optimum reagent ion yield (Fig. S1 in the Supplement), with nearly 1 order of magnitude lower flows than polonium or X-ray-based ion sources typically use. The residence time inside the reactor under these standard conditions is ~ 10 ms.

Modeled flow velocities in the Vocus AIM IMR (Fig. 1) were used to optimize the flow patterns inside the reaction cell. The velocity field shows the intersection of the reagent ion jet with the sample flow and was optimized to minimize the contact of sample gas with reactor surfaces as well as to prevent turbulent eddies near the gas expansion region. The gas flow dynamics were modeled with the open-

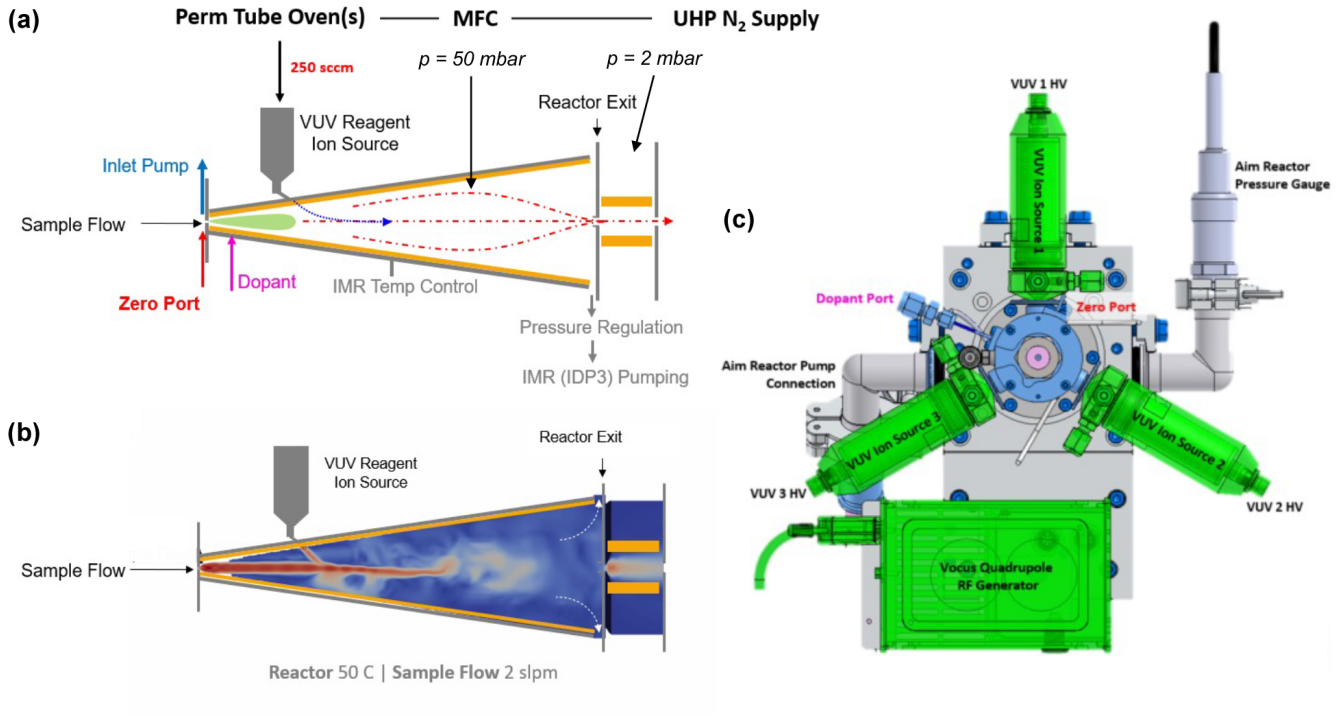

Figure 1. **(a)** Diagram of the Vocus AIM reactor showing the conical design and relative locations of the sample and reagent ion additions. **(b)** Cross-sectional view of modeled flow velocities in the AIM–IMR, showing optimized intersection of the reagent ion and sample stream flows and limited contact of the sample gas with surfaces. Dopant flow was not considered for the CAD calculation. **(c)** Key components of the Vocus AIM reactor.

source computational fluid dynamics (CFD) software OpenFOAM v8 (https://openfoam.org/, last access: 13 September 2024) using a customized solver (https://github.com/pasturm/rhoReactingPimpleFoam, last access: 13 September 2024) to simulate supersonic flow in a vacuum with mixing of different gases. The final geometry is constrained by machinability (finite tool dimensions), while also minimizing the response time and reducing reactive and ion wall losses.

2.2 Reagent ion generation

Compact VUV ion sources generate reagent ions by converting photons from a VUV lamp (UV lamp krypton DC PID PKS 106, Heraeus) at two wavelength bands corresponding to energies of ~ 10.0 and 10.6 eV into the desired reagent ions (Ji et al., 2020; Breitenlechner et al., 2022). As in prior work, we utilize a primary photo-absorber (e.g., benzene) as a source of photoelectrons and directly formed cations to generate subsequent reagent ions. Permeation tubes are held at 80 °C in a compact oven and deliver constant amounts of corresponding photo-absorber and reagent ion precursor into the 0.250 slpm ultrahigh purity (UHP) nitrogen stream. Gaseous benzene (C_6H_6, Sigma Aldrich, $\geq 99.9\,\%$) delivered from the permeation tube enters the VUV lamp housing and is photoionized (with an absorption cross-section of 4×10^{17} cm^2 molec.$^{-1}$ and ionization potential = 9.24 eV), yielding $C_6H_6^+$ and photoelectrons (Lavi et al., 2018). By mixing benzene with trace methyl iodide (CH_3I, Sigma Aldrich, 99.8 %), bromoethane (C_2H_5Br, Sigma Aldrich, $\geq 99\,\%$), or nitric acid (HNO_3, Sigma Aldrich, $\geq 65.6\,\%$), various anions such as I^-, Br^-, or NO_3^- are generated alongside $C_6H_6^+$ following Reactions (R1) and (R2) and are introduced into the Vocus AIM reactor. The compatibility between multiple ion chemistries in the AIM system is determined by whether a generated reagent ion can detect the neutral precursors from any other attached ion source. A small aperture at the exit of the illuminated region of the ion source prevents back-diffusion of sample air into the primary ionization chamber.

$$C_6H_6 + h\nu \rightarrow C_6H_6^+ + e^- \quad \text{(R1)}$$

$$CH_3I + e^- \rightarrow CH_3 + I^- \quad \text{(R2)}$$

By manipulating the above mechanisms, other reagent ions can be readily produced in high abundance and high purity. Cl^- reagent ions can also be produced by introducing 0.250 slpm of UHP nitrogen through the permeation tube oven containing the pure dichloromethane (CH_2Cl_2, Sigma Aldrich, $\geq 99.8\,\%$) permeation tube. Once formed, anion reagent ions mix with the sample flow in the main reaction chamber and ionize the compounds of interest (M) through the reactions described in Reactions (R3) and (R4), with X being I^-, Br^-, Cl^- or $(HNO_3)_nNO_3^-$ ($n = 0, 1, 2$).

$$M + X \rightarrow M...X \quad \text{(R3)}$$

$$M + X \rightarrow M\text{-}H + HX \quad \text{(R4)}$$

To generate ammonium ions, we irradiate gaseous acetone with VUV light, which results in self-protonated acetone Reaction (R5) and directly reacts with the acetone molecules yielding protonated acetone dimers (Reaction R6; Dong et al., 2022). A continuous flow of NH_3, typically a few standard cubic centimeters per minute (i.e., $[NH_3] > 100$ ppm), from a 1 % gas cylinder (in nitrogen) can be introduced directly into the VUV source along with the acetone (Fig. 1). NH_3 molecules react with the protonated acetone yielding acetone–ammonia adducts that can be used for subsequent ionization in the main reaction chamber (Reaction R7). If the concentration of NH_3 is lower than 100 ppm, multiple ionization processes might occur (e.g., acetone dimers or charge transfer), which would complicate the mass spectrum analyses.

$$2(C_3H_6O) + h\nu \rightarrow C_3H_7O^+ + C_3H_5O^- \quad \text{(R5)}$$

$$C_3H_7O^+ + C_3H_6O \rightarrow C_6H_{13}O_2^+ \quad \text{(R6)}$$

$$C_3H_7O^+ + NH_3 \rightarrow C_3H_6O{-}NH_4^+ \quad \text{(R7)}$$

Similar to anion reagent ions, these positive ions can ionize the compounds of interest through either adduct formation or proton transfer or, in the case of benzene, charge transfer. At pressures of 50 mbar, most chemical ionization reactions occur via ligand switching reactions involving the analyte and hydrated reagent ions.

To minimize the effect of water vapor during the ionization process inside the IMR, a water vapor control system consisting of a regulated flow of a dopant (i.e., organic compound) can be injected directly into the IMR (Fig. 1). By replacing water with a stable concentration of the dopant, a stable ion distribution is obtained across the entire range of relative humidity (RH; further discussed in Sect. 3.2).

2.3 Vacuum interface and analyzer

At the exit of the Vocus AIM reactor, product ions are sampled through a 1 mm orifice into the differentially pumped vacuum interface. The efficiency with which the ions at the end of the reactor are sampled depends primarily on the ratio of the sample flow that exits through the orifice relative to the flow towards the vacuum pump evacuating the reaction chamber. This flow split is in turn also dependent on the reactor pressure but is typically ~ 0.5 slpm. After entering the next stage of the interface, an RF-only (radio frequency) quadrupole ion guide efficiently focuses the analyte ions into a narrow beam, leading to the net removal of the neutral molecules by a vacuum pump (Ebara PDV 500). Typical RF amplitudes of 100 V_{p-p} are sufficient to focus most ions without significant ion activation for the iodide–water adduct, where the iodide–water adduct is a very weakly bound complex that is known to respond to transfer through vacuum interfaces relative to its known thermodynamic distribution. In general, reagent ions and analyte ions that are very weakly bound to the reagent ions (e.g., water clusters with a binding energy of 10 kcal mol^{-1}; Caldwell et al., 1989) are often observed to deviate from the thermodynamic distribution with RF amplitudes > 50 V_{p-p}. This is not entirely problematic, as the binding energy of these complexes is usually too weak for sensitive detection even at the weakest transfer conditions. For typical analytes with moderate binding energies (e.g., iodide–formic acid adducts), no significant declustering is observed at RF amplitudes < 125 V_{p-p}. We find that the optimal voltage gradients in the first quadrupole region are typically all 0 V between electrodes, as ions are focused on the radial direction efficiently by the RF but transported axially by the gas flow. This ensures that ions are transmitted with the lowest-possible added energy into the next stage of the vacuum interface. The rest of the differentially pumped interface is pumped by a single split flow turbo pump (Pfeiffer SF270) and consists of an additional segmented quadrupole ion guide held at 10^{-2} mbar that transfers energetically cooled ions into a lens stack held at 10^{-5} mbar before an orthogonal extraction in a time-of-flight mass analyzer (Tofwerk Vocus CI-TOF 2R) operated at $< 10^{-6}$ mbar The instrument was configured to measure a mass-to-charge (m/Q) range of 1–900 Th (12 kHz extraction frequency) with a mass resolving power of 10 000–11 000 for the experiments described herein.

2.4 Flow tube oxidation experiments

Ozonolysis/OH-radical-initiated oxidation of α-pinene ($C_{10}H_{16}$) experiments were performed under dry conditions, at room temperature, and at atmospheric pressure in a flow tube reactor. The reactor consisted of a ~ 6 L Pyrex glass tube (80 mm i.d., × 120 cm length). The total flow rate of dry synthetic air (N_2/O_2 80 : 20) was set at 5.5 slpm, giving an average residence time of 70 s. A mixing ratio of 60–70 ppb of ozone generated by an ozone generator (Fisher Scientific, SOG-1) was continuously injected into the flow tube. A mixing ratio of 200 ppb α-pinene was introduced from a homemade gas cylinder (40 ppm in UHP N_2). The sample was immediately sampled into the reactor at a sample flow rate of 1.8 slpm with the excess flow going to exhaust.

2.5 Calibration

To measure the instrument's sensitivity, we calibrated the reactor using different compounds, each selected to follow general structural selectivity rules for each ion chemistry. For example, no sensitivity for xylene is reported for negative ions, as negative ions like iodide do not detect xylene with any significant sensitivity. To calibrate benzene cations, we used a multicomponent gas (Apel Riemer Environmental

Inc) containing a mixture of hydrocarbons and ketones (Table S1 in the Supplement). An internal calibration gas system consisting of two mass flow controllers (Bronkhorst, capacity 30 and 2000 sccm) and a mixing volume diluted a flow of 10 sccm of the gas standard into a carrier flow of 2000 sccm of UHP nitrogen resulted in a final mixing ratio of 5 ppb for each compound present in the gas mixture. For iodide anions and protonated acetone dimers, a liquid calibration system (LCS v2; Tofwerk) was used to form standard concentrations of lower volatile species not compatible with gas cylinders. By introducing a continuous flow of liquid with a known concentration into a nebulizer and aluminum evaporation chamber, the LCS provides a continuous, calibrated gas-phase concentration to the instrument. The evaporation chamber of the LCS was set to a temperature of 150 °C, with a UHP nitrogen flow rate of 2000 sccm thereby slightly overflowing the sample inlet. For the lower volatility compounds, we cannot rule out losses in the LCS but find that collision-limited sensitivities between positive and negative ion modes agree well within experimental uncertainty. Aqueous solutions with concentrations ranging from 5 to 50 µM and liquid flow rates of 10 µL min^{-1} were used to reach target concentrations in the low parts per billion range for each molecule and maintain constant water vapor concentrations during calibration. Ammonia concentrations were generated using a gas standard and independently compared to a cavity ring-down spectroscopy gas analyzer (Picarro Model G2508) to validate the sensitivity and linearity of protonated acetone dimers to ammonia (Fig. S2).

Instrument backgrounds and detection limits are determined by measuring UHP nitrogen at the entrance of the reactor. We note that measuring the total background should include any background measurement of sampling inlets, but such characterization and best practices for sampling are beyond the scope of this paper and are discussed in detail elsewhere (Palm et al., 2019; Riva et al., 2019). We therefore report detection limits using UHP nitrogen overflowing the inlet using the zero port, which introduces zero gas only to the high-pressure (atmosphere) side of the critical orifice at the entrance of the reactor. We purged the instrument before and after the calibration experiment for 10 min with UHP nitrogen to determine the instrument background count rates. As reported in detail previously (Palm et al., 2019), during a background measurement the reactor walls are pushed out of equilibrium by the incoming clean air. This perturbation can impart a transient effect on different compounds depending on primarily volatility. For volatile and extremely low volatility compounds, the response to a step change in concentration (introduction of zero air) is close to instantaneous (< 100 ms) due to negligible adsorption (sticking rate) for the volatile species and effectively infinitely slow evaporation rates from walls for the lowest-volatility compounds (irreversible loss). For background determinations, the most challenging group of compounds are intermediate and semi-volatile compounds that readily respond to changing inlet conditions and partition back and forth between the reactor walls and the reactor flow. In laboratory conditions or at ground sites where temporal changes are often only slowly changing, we use dry UHP N_2 to replace the incoming sample air for 1 min. As noted in prior work, under more dynamic environments the duration and frequency of instrument background measurements should be decreased and increased to match the respective temporal changes that are to be measured.

3 Results and discussion

3.1 Vocus AIM time response

Real-time measurements require a fast time response to report temporal trends in measured concentrations accurately. For many compounds, the time response can approach that of the volumetric time response of the reactor (3–30 ms); however, for semi-volatile (i.e., sticky) compounds, the time response is often observed to be much slower than the volumetric time constant as interaction with the reactor walls results in smearing of the concentration over time. The primary interaction of the analyte and the reactor walls defines the response time at constant temperature, pressure, and flow. Therefore, optimizing the shape and the materials of the wetted surfaces is critical to maintaining a fast response. The Vocus AIM reactors' conical design notably improves the time response by ensuring that the walls get further and further from the exit orifice along the length of the reactor. This shape increases the probability that vapors that have interacted with the wall are pumped away instead of being ionized and transferred into the mass analyzer. It also ensures that in the region of the primary expansion, the recirculation eddies do not have significant space to form, allowing a faster equilibration time at the entrance of the reactor (Fig. 1). To accurately measure dynamic changes in concentration, particularly for low-volatility species like oxidized organics, inorganic acids, and reactive species, cPTFE is chosen as the reactor wall material. Teflon®-based materials have on average the weakest interaction with most organic and inorganic compounds (Morris et al., 2024) and are therefore a good choice for the reactor walls. cPTFE in particular is chosen as its conductivity prevents surface charge-up of the reactor walls, which would result in unstable or slowly equilibrating ion signals. We evaluate the performance of the reactor using molecules that represent a worst-case scenario i.e., have a high surface affinity and interact strongly with the walls of the reactor. In Fig. 2 we compare the measurement of nitric acid in the AIM reactor with iodide adduct ionization from other IMR reactors (Lee et al., 2018; Palm et al., 2019) with different approaches to improve the time response, notably comparing a very short stainless steel tubular reactor and a larger flow tube reactor with laminarizer and sheath flow operated at reduced pressure. To quantitatively compare

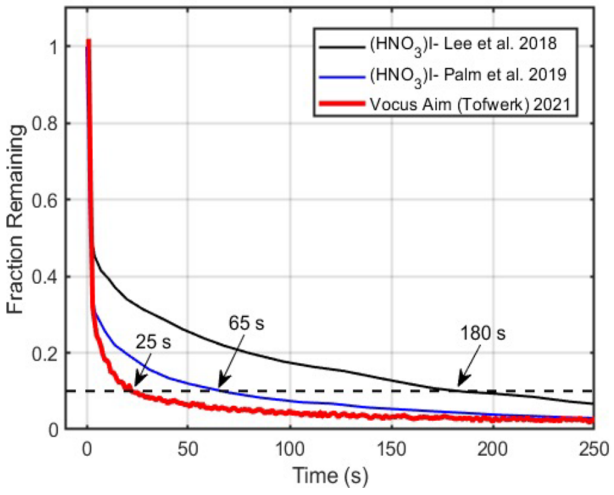

Figure 2. Time response to nitric acid of the Vocus AIM IMR compared to the previous IMR designs found in the literature.

the time responses of these different reactors, we measured the decay time, defined as the duration required for the signal to fall below 90 % of its peak value after the source of nitric acid is removed. While the response time of the Vocus AIM reactor is not instantaneous, it is faster by roughly a factor of 3–4 than previously published medium-pressure reactors. The improved time response is most critical for ensuring that the memory effect in the reactor is minimized, crucial for applications where fast transients need to be quantified, for example in mobile laboratories, aircraft, or flow tube reactors.

3.2 Water vapor control and suppression

A major limitation of chemical ionization reactors operated at elevated pressure is that water vapor can strongly impact the net reaction mechanism and reagent ion distribution, resulting in sensitivities that are humidity-dependent (W. Zhang et al., 2023; Y. Zhang et al., 2023), as shown in Fig. S3 for the reagent ion distribution. Such changes pose considerable challenges for accurate quantification of species in conditions where humidity is variable. The sensitivity to a given compound will depend on whether water vapor competes with it for the reagent ion, i.e., lowering the sensitivity, or whether the presence of water molecule offers a loosely bound third body to stabilize the adduct by removing the excess energy after the M–reagent ion collision, thereby increasing sensitivity. While post-measurement correction can be performed, it is labor-intensive and prone to errors, as each compound essentially has a unique humidity dependence. To overcome this fundamental drawback, the Vocus AIM reactor introduces a system to mitigate water vapor dependencies using a dopant. The dopant effectively replaces water vapor, the dominant ligand in the switching reaction involving the reagent ions and the analyte molecules. A dopant could in principle be any molecule that binds (forms an adduct) with the reagent ion more strongly than the reagent ion and water. In this way, the dopant can displace the water molecules that would normally be attached to the reagent ions with a compound that is not variable or present in significant concentrations in the sample gas. The following equations show the modified reaction mechanism in the presence of a dopant (D) in the case of iodide anions.

$$\mathrm{I}(\mathrm{H_2O})n^- + \mathrm{M} \rightarrow \mathrm{IM} + (\mathrm{H_2O})n \quad (1)$$

$$\mathrm{ID} + \mathrm{M} \rightarrow \mathrm{IM} + \mathrm{D} \quad (2)$$

The modified reaction mechanism no longer significantly depends on varying water vapor conditions as long as the dopant molecule is present in sufficiently high concentrations to replace most of the water ligand. In the above chemical ionization mechanism for iodide anions, the challenge can be to choose a suitable dopant. While the dopant must efficiently displace the water that is bound to iodide, it is also desirable for the binding energy to be close to that of water. This ensures that the net chemical ionization selectivity remains nearly unchanged compared to the dopant-free conditions. If a dopant with a very high binding energy is selected, it will introduce a binding energy ionization threshold, which will significantly change the selectivity of the given ion chemistry by essentially removing all weakly bound adducts from the spectra. Here we investigate three different dopants including acetonitrile, methanol, and acetone. These compounds weakly interact with iodide anions and have a high vapor pressure, which facilitates their easy introduction into the reactor. This is typically achieved using a mass flow controller (MFC; Bronkhorst Low Delta P, 30 sccm) that draws from the headspace of a liquid reservoir, effectively minimizing the net dilution (net sample dilution ~ 1 %).

For each of the evaluated dopants, stable concentrations of formic, nitric, and acrylic acids were introduced into the entrance of the reactor. The incoming air was humidified with two mass flow controllers, one delivering dry nitrogen and the other passing dry nitrogen through a water bubbler held at room temperature. The ratio of the two mass flow controllers was programmatically changed to simulate changes in sample humidity for each dopant flow rate. Figure 3 illustrates how the systematic introduction of each of these dopants at different mass flow rates influences the reactor's detection efficiency for nitric, formic, and acrylic acids under changing humidity levels (0 %–100 % relative humidity at 25 °C). These compounds were selected as characteristic compounds for the iodide adduct system, each demonstrating a distinct sensitivity dependence on humidity that follows the changes in the water–iodide cluster distribution (Lee et al., 2014).

Under dopant-free conditions, we expect nitric acid to first sharply increase from dry conditions to humid conditions, followed by a plateau at water vapor partial pressures of ~ 0.25 mbar. This can be attributed to nitric acid's high binding enthalpy with I^- and a small (1 kcal mol^{-1}) difference

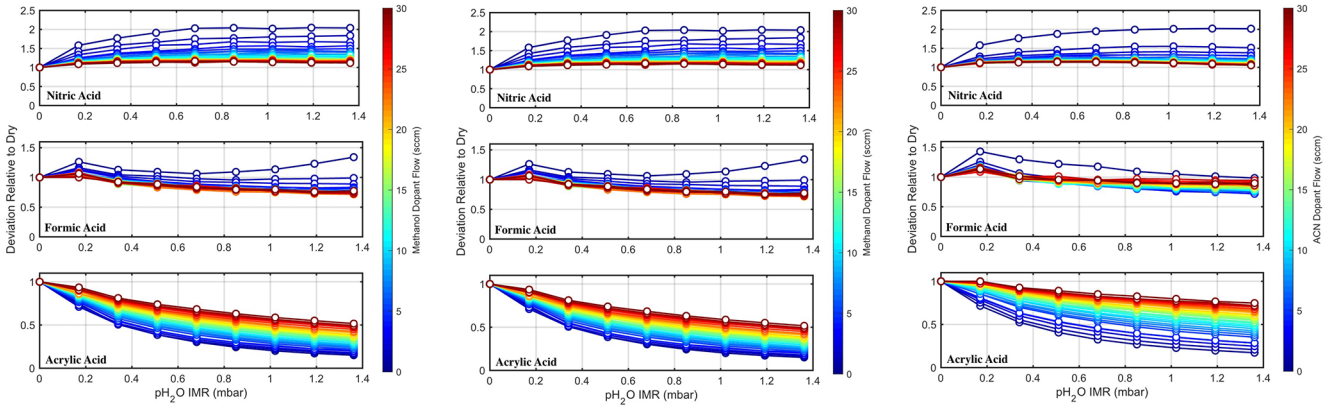

Figure 3. Impact of the relative humidity on the sensitivity of nitric acid, formic acid, and acrylic acid as a function of different dopant concentrations (dopants: acetone, methanol, and acetonitrile). The x axis displays the partial pressure of water, corresponding to higher humidity levels within the reactor (0 %–100 % humidity). The color gradient indicates the increasing flow of specific dopants.

from the binding enthalpy to $I(H_2O)^-$, which is sufficiently compensated by the kinetic stabilization from the increased number of vibrational modes due to the addition of the water molecule (Lopez-Hilfiker et al., 2016). In the case of acrylic acid, the sensitivity as a function of water vapor concentration falls rapidly following the availability of unhydrated iodide anions. With increasing water vapor concentrations, the weak binding energy between acrylic acid is not enough to overcome the competition with water for the bare iodide ions. Formic acid is between these two extremes, initially stabilized by the presence of water but ultimately in competition with water for iodide ions as the second water cluster forms, reducing the sensitivity at higher absolute humidity.

In the doped conditions, the humidity dependencies are significantly reduced for all molecules. The dopant and humidity scans demonstrate the net effect of the different dopants for each molecule as a function of the total dopant flow introduced. While methanol and acetone to a certain extent shift the reagent ion distribution, they are not present in high-enough concentrations to fully displace the water and stabilize the reagent ion distribution against changes driven by humidity changes. Acetonitrile, on the other hand, demonstrates a significant shift in reagent ion distributions and a significant damping of the humidity dependency, particularly at flows greater than ~ 20 sccm. With acetonitrile as the dopant, the change in sensitivity across the humidity range is reduced to a deviation of < 20 % relative to dry conditions for all model compounds, more for formic acid and nitric acid (< 10 %). From the relative flattening of the humidity dependence, for iodide anions (Caldwell et al., 1989) acetonitrile emerges as the most efficient dopant tested, reducing sensitivity variability across most analytes to a deviation that becomes negligible for ambient analysis.

While this example focused on the dopant's presence in the reaction mechanism for iodide anions, the same concept holds for any adduct-forming ion, including Br^- and Cl^-. For example, when generating protonated ammonium ions in the presence of acetone, the formation of the C_3H_6O–NH_4^+ adduct with acetone itself acts as a dopant and greatly suppresses the water vapor dependency, as demonstrated in Fig. S4. Where ammonium ions alone exhibit order-of-magnitude humidity dependencies when operated at elevated pressure, this variability is reduced to < 30 % with significant acetone present as the dopant (Canaval et al., 2019; Xu et al., 2022; Li et al., 2023), greatly simplifying analysis.

3.3 Sensitivity and limits of detection

Sensitivities for a variety of compounds were evaluated for each ion chemistry to quantify the overall instrument performance. Calibrations were typically done at one or two different concentration steps in the range of a few parts per billion by volume. Sensitivities were normalized to the number of recorded reagent ions measured at the detector, which provides a straightforward method for correcting for any absolute fluctuations in the instrument's response over time, and referenced to a recorded total reagent ion current of 10^6 ions s^{-1}. Typical reagent ion currents measured on the Vocus AIM reactors are between 3 and 6×10^6 ions s^{-1} for iodide anions and benzene cations. Results from the calibration experiments are summarized in Table 1, organized by reagent ion. The compounds for calibration were specifically selected based on their selectivity for each reagent ion and their relative ease of producing stable concentrations. A diverse range of hydrocarbons, reactive nitrogen species, organic compounds (with various volatilities), and inorganic acids can be detected, with high sensitivities often greater than ~ 10 counts s^{-1} $pptv^{-1}$ per (10^6 reagent ions). The sensitivity of the Vocus AIM reactor does not necessarily surpass that of previous low- and medium-pressure reactors (Lee et al., 2014, 2018; Ye et al., 2021; Xu et al., 2022) in an absolute sense, however, the sensitivity is in the same approxi-

mate range and reaches the extremely low limit of detections (LoD) ranging from 0.1 to 5 ppt for most compounds. LoD measurements were performed by introducing 2 slpm of dry UHP N_2 (i.e., background measurement) for 10–15 min. The LoD was estimated using Tofware and calculating the Allan variance (i.e., the stability of the signal over time). Finally, the LoD corresponds to 3 standard deviations (σ) of the Allen variance and is determined as a function of integration time estimation. As an example, using acetone dimers as reagent ions, the LoD for ammonia is about 10 ppt (1 min averaging), which is 1–8 times lower than previously reported for this compound (You et al., 2014; Dong et al., 2022; Schobesberger et al., 2023). Additionally, using a benzene cation as a reagent ion, the LoD for monoterpenes (e.g., 0.2 ppt for α-pinene at 1 min) can even surpass conventional PTR techniques, including the Vocus PTR (i.e., 4 ppt for α-pinene at 1 min; Krechmer et al., 2018) and giving similar results as the FUSION PTR (i.e., 0.1 ppt at 1 min; Reinecke et al., 2023).

The absolute sensitivity of the instrument depends fundamentally on the reaction time and collision frequency (pressure) as well as the absolute number of generated reagent ions introduced into the reactor. Figure 4a shows the dependence of the measured sensitivity of levoglucosan on the reactor pressure. By increasing the pressure from 35 to 75 mbar the sensitivity of the instrument can be increased by a factor of ~ 4, which is consistent with the increase expected based on reaction time and collision frequency. Operating at higher pressures can be beneficial in pristine or highly diluted environments, where the concentrations of target compounds can reside in the sub-parts-per-trillion (sub-ppt) range. A nominal operation pressure of 50 mbar provides a good balance between sensitivity and linear range that under typical conditions extends to $\sim$ 100–200 ppbv depending on the analyte (Fig. 4b). This allows the standard conditions (which are a compromise between sensitivity and linear range) of the Vocus AIM reactor to operate equally well in pristine and polluted environments with the same configuration. In highly polluted environments where the total detectable mass concentrations greatly exceed the linear range of the instrument, reagent ion normalization can compensate for up to 50 % of reagent ion depletion before normalization errors begin to accumulate. In such conditions, the incoming sample flow would need to be diluted to maintain concentrations within the normalization range.

Finally, taking advantage of the improved time response and the possibility of operating more than one VUV lamp on the Vocus AIM reactor (Fig. 1), a fast switch between different ion chemistries at up to 2 Hz is now possible, as shown in Fig. S5. This valuable feature allows the Vocus AIM reactor to extend the variety of compounds detected by one instrument within a single polarity, as the mass analyzer used in this study had polarity-switching timescales of 5–10 min.

3.4 Vocus AIM performance for atmospheric applications

To evaluate the bulk detection capabilities of Vocus AIM, we measured oxidation products from the OH/O_3-initiated oxidation of α-pinene using a steady-state flow tube setup. This reaction mechanism was chosen because it is a well-studied system resulting in a suite of oxidation products spanning a wide range of functionalities. Additionally, it generates molecules with a wide range of molecular masses, from lightly oxidized monomers to heavily oxidized dimers. In total, four AIM reagent ion chemistries, namely NH_4^+, Cl^-, I^-, and NO_3^-, were used to investigate their relative detection efficiency (selectivity) towards produced oxygenated volatile organic compounds (OVOCs). AIM offers an ideal method for evaluating ion chemistries as it ensures uniformity in the introduction of all reagent ions and utilizes the same analytical instrument for comparison. This approach effectively eliminates the instrument-to-instrument variability, thus providing a highly direct and unbiased comparison of ion chemistry and detection efficacy for a variety of mixed organic compounds.

RO_2 radicals generated from the combined ozonolysis and OH radical reaction of α-pinene can further react, yielding mixed oxidation products during the reaction time in the flow tube. Among the different RO_2 radicals formed, $C_{10}H_{15}O_{>3}$ and $C_{10}H_{17}O_{>2}$ were detected by the different reagent ions used. While the mass spectra are generally similar between the different reagent ion chemistries, there are some notable differences in the detection efficiencies. NO_3^--ion-based chemistry is by far the most selective of the reagent ions tested. A smaller group of compounds was detected, with a particular inclination towards the most heavily oxidized monomers and gas-phase dimer species. The variable selectivity of the different ion chemistries is demonstrated in Fig. 5, organized by the increase in reagent ion selectivity. NH_4^+ and Cl^- are the least selective ions evaluated, highlighted by the large ion signal intensity of compounds $m/Q < 100$ Th (least oxidized) and the largest number of absolute compounds detected. While the sensitivity to less oxidized compounds is limited to the less selective reagent ions (i.e., NH_4^+ and Cl^-), more-selective reagent ions excel at detecting the lower concentration of more oxidized compounds. The selectivity of the reagent ion plays a pivotal role in limiting the backgrounds and potential isobaric interferences that might hamper the detection of the compounds of interest. With the AIM reactor and the right selection of reagent ion, even the most highly oxidized RO_2 radicals (e.g., $C_{10}H_{17}O_7$ and $C_{10}H_{15}O_8$) and dimeric products (e.g., $C_{19}H_{28,30}O_x$ and $C_{20}H_{30,32}O_x$) can be identified under relevant atmospheric conditions, highlighting the very high sensitivity and versatility of the Vocus AIM reactor.

To demonstrate the bulk detection properties of the different reagent ion chemistries more clearly, we categorized each compound according to its estimated volatility. Due to

Table 1. Sensitivities (pptv) normalized by 10^6 detected reagent ions for different ion chemistries used with the Vocus AIM reactor.

Compounds	Reagent ion	Sensitivity (counts s^{-1} $pptv^{-1}$ per (10^6 reagent ions))	LoD (1 min)
Toluene	Benzene (+)	7.8	0.4
m-Xylene	Benzene (+)	7.6	0.2
1,2,4-Trimethyl benzene	Benzene (+)	7.5	0.2
α-Pinene	Benzene (+)	6.8	1.4
Methyl ethyl ketone	Acetone–ammonia (+)	5.0	4.8
Ammonia	Acetone dimer (+)	1.5	1.0
Methyl amine	Acetone dimer (+)	1.2	10
Ethyl amine	Acetone dimer (+)	1.6	1.0
Dimethyl amine	Acetone dimer (+)	2.2	1.0
Diethyl amine	Acetone dimer (+)	2.6	1.0
Trimethyl amine	Acetone dimer (+)	2.5	4.0
Triethyl amine	Acetone dimer (+)	5.0	2.0
Formic acid	Iodide (−)	2.0	0.8
Levoglucosan	Iodide (−)	6.0	0.1
Chlorine	Iodide (−)	5.5	3.0
Nitric acid	Iodide (−)	4.3	5.0
Fluoric acid	Iodide (−)	3.0	10
Iodine	Bromide (−)	3.0	2.0

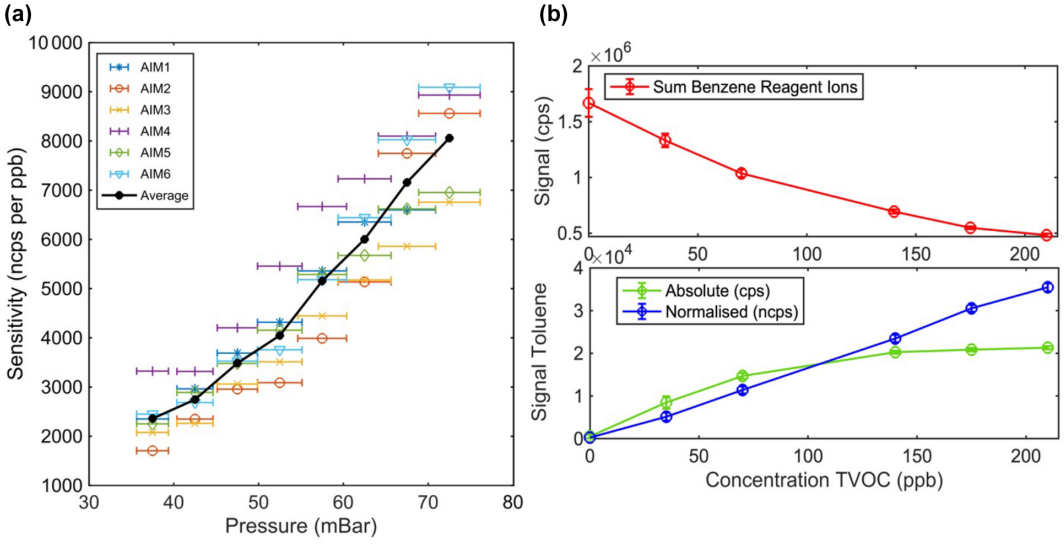

Figure 4. Panel **(a)** presents the sensitivity dependance on the IMR pressure. The solid line represents the average sensitivity from six distinct Vocus AIM instruments, each normalized to 1 million reagent ions. Individual sensitivity measurements for each reactor are depicted as unique symbols. The error bars provide an estimate of the pressure gauge measurement uncertainty within 5 % of error. Panel **(b)** shows the evolution of the sum of the reagent ions for benzene cation chemistry (upper panel) and the ion signal intensity of toluene with and without normalization to reagent ions under a wide range of concentrations (lower panel).

the lack of authentic standards measuring the vapor pressure of oxygenated organic molecules (OOMs), this remains an analytical challenge. To overcome this problem, model calculations have been developed to estimate the vapor pressure using, for example, structure-based estimations and formula-based estimations. The volatility basis set (VBS) framework has been established by Donahue et al. (2011) and is widely used in atmospheric chemistry to estimate the volatility of products measured by mass spectrometry techniques. The VBS parameterization is useful for classifying the wide range of OOMs into multiple volatility groups, including extremely low volatility organic compounds (ELVOCs) and

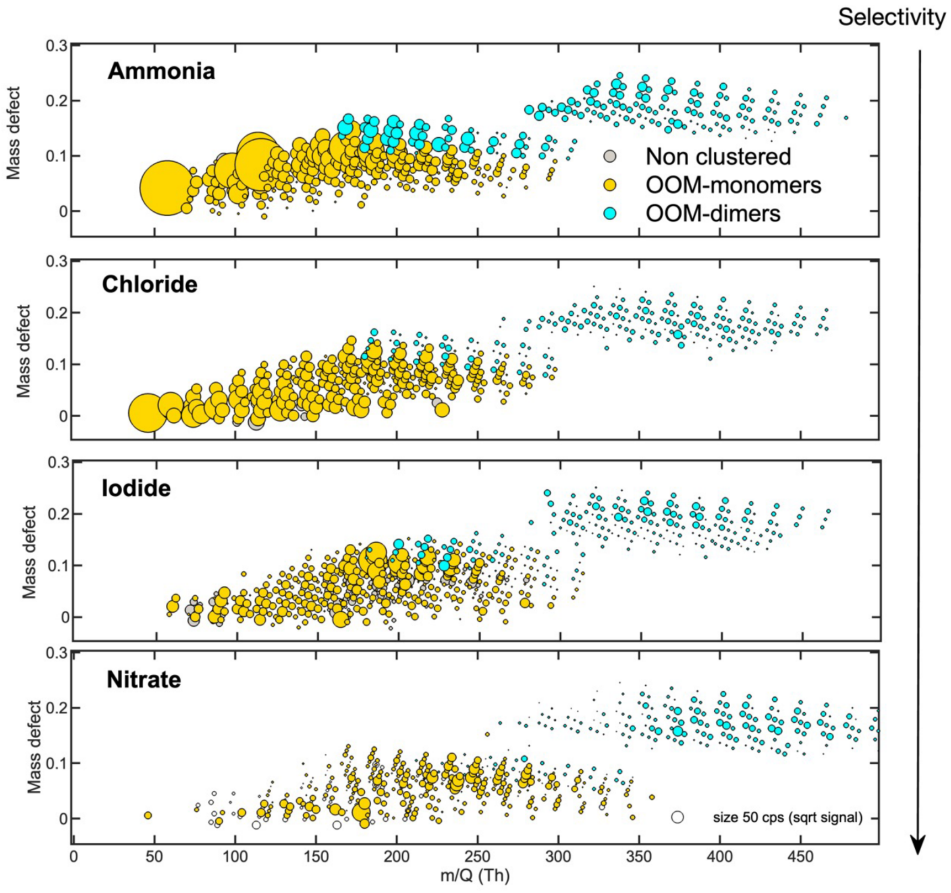

Figure 5. Mass defect plots of organic compounds measured by the Vocus AIM reactor using ammonia, chloride, iodide, and nitrate ion chemistries generated via the O_3/OH-initiated oxidation of α-pinene. The x axis represents the mass-to-charge ratio of the neutral analyte; the y axis represents the corresponding mass defect, which is the difference between their exact mass and nominal mass; and the size of the circle represents the square root of the signal intensity measured for each ion.

low-volatility organic compounds (LVOCs), based on their effective saturation concentration (C^*; in units of $\mu g\,m^{-3}$). In this work, we apply the VBS parameterization optimized by Li et al. (2016),

$$\log_{10}C^*(298\,K) = \left(n_C^0 - n_C\right)b_C - n_O b_O - 2\frac{n_C n_O}{(n_C+n_O)}b_{CO} - n_N b_N - n_S b_S, \quad (3)$$

where n_C, n_O, n_N, and n_S are the number of carbon, oxygen, nitrogen, and sulfur atoms of the specific molecule, separately; n_C^0 is the reference carbon number; b_C, b_O, b_N, and b_S are the contribution of each atom to $\log_{10}C^*$,; and b_{CO} is the carbon–oxygen non-ideality. The b coefficient values can be found in Li et al. (2016). In this study, all oxidation products generated from the OH/O_3-initiated oxidation were grouped into six volatility regimes: ultralow-volatility (ULVOCs, $C^* < 10^{-8.5}\,\mu g\,m^{-3}$), extremely low volatility (ELVOCs, $10^{-8.5} < C^* < 10^{-4.5}\,\mu g\,m^{-3}$), low-volatility (LVOCs, $10^{-4.5} < C^* < 10^{-0.5}\,\mu g\,m^{-3}$), semi-volatile (SVOCs, $10^{-0.5} < C^* < 10^{2.5}\,\mu g\,m^{-3}$), and intermediate-volatility organic compounds (IVOC, $10^{2.5} < C^* < 10^{6.5}\,\mu g\,m^{-3}$), as well as VOCs ($10^{6.5} < C^*\,\mu g\,m^{-3}$), based on VBS.

Figure 6 illustrates the measured range of oxidation products generated by the hydroxyl radical and ozone reaction with α-pinene. These products were analyzed using one mass spectrometer with the AIM reactor setup employing various ionization chemistries. Therefore, unlike other studies (Riva et al., 2019; Li et al., 2023) this study utilizes a single instrument, thereby reducing uncertainties associated with the calibration and settings of different instruments, as well as with the conditions during sample collection. The total signal in each volatility bin represents the sum of the signal intensity of OOMs within the volatility range. Organic compounds with C^* of $< 10^{-1}\,\mu g\,m^{-3}$ made up the largest signal contributions for the Vocus AIM using NO_3^--ion-based chemistry (Table S2). This observation is consistent with the conventional atmospheric pressure using NO_3^- as the reagent ion and indicates that the design of the Vocus AIM reactor allows the detection of ELVOC and ULVOC (Riva et al., 2019; W. Zhang et al., 2023; Y. Zhang et al., 2023). This is a

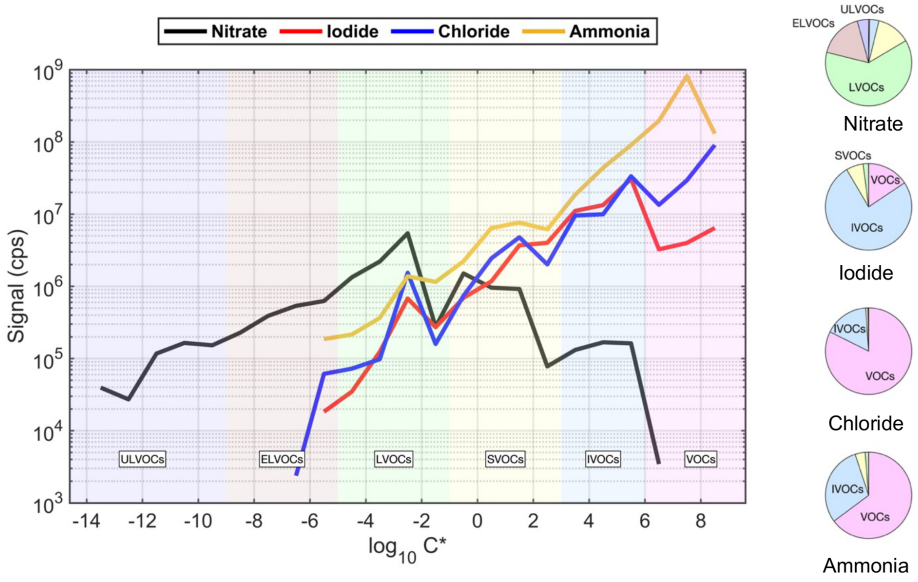

Figure 6. Volatility distribution comparison for organic compounds detected by the Vocus AIM using nitrate, iodide, chloride, and ammonia ion chemistries. Ion intensity represents the cumulative signal recorded for each ion chemistry. The background colors represent the saturation concentration (C_{sat}) in the range of ultralow-volatility (ULVOCs, purple), extremely low volatility (ELVOCs, brown), low-volatility (LVOCs, green), semi-volatile (SVOCs, yellow), intermediate-volatility (IVOCs, blue), and volatile organic compounds (VOCs, pink). The pie charts represent the corresponding contributions of VOC, IVOC, SVOC, LVOC, ELVOC, and ULVOC classes from the O_3/OH-initiated oxidation of α-pinene.

substantial improvement for the atmospheric science community, as measurement of such species is solely possible with the use of atmospheric pressure interfaces that can be associated with sensitivity fluctuations (e.g., the RH effect). As demonstrated previously (Riva et al., 2019), I^--ion-based chemistry detects oxygenated compounds with C^* ranging from 10^{-5} to 10^5 µg m^{-3}, which corresponds to OOMs and starts to be less sensitive to oxygenated compounds having fewer oxygen atoms that are included in the IVOC fraction. While Cl^- and NH_4^+ can also measure OOM with C^* as low as 10^{-5} µg m^{-3}, the weak selectivity of these ion-based chemistries allows them to measure a wider range of compounds (i.e., IVOCs and VOCs). IVOCs and VOCs generally include less-oxygenated VOCs with shorter carbon skeletons and comprise the main fraction of organics formed from the oxidation of pinene (Isaacman-VanWertz et al., 2018). We stress here that while it was not possible to detect ULVOCs and ELVOCs using I^--, Cl^--, or NH_4^+-ion-based chemistries, it is purely a selectivity limitation of the more general reagent ions and not of absolute sensitivity, as all the tested reagent ions have similar overall absolute sensitivities. Nitrate reagent ions benefit from the high selectivity, which also manifests in a lower background signal, therefore enabling nitrate anion chemistry to detect ULVOCs and ELVOCs. With the significantly lower background concentrations of nitrate ions, the detection of compounds at extremely low concentrations (as low as 10–100 ppqv) becomes possible.

Differences in the contribution of these compound groups (i.e., relative signal contribution to total OOMs) compared to previous work could be due to different sensitivities of the instruments towards organic compounds with varying oxidation extents (Riva et al., 2019). In addition, experimental conditions (e.g., RH, temperature, precursor concentration) and setup (flow tube reactor, atmospheric simulation chambers) can greatly impact the distribution of OOMs retrieved by MS techniques. By carefully selecting the type of reagent ion, the combined volatility distribution can cover VOCs to OOMs, with varying O : C ratios and volatility ranges (Fig. 6), all within a single instrument. The Vocus AIM can therefore provide a more complete picture of the volatility distribution of gaseous organic and inorganic compounds found in the atmosphere.

4 Conclusions

The primary goal of this work was to evaluate the performance of the newly designed Vocus AIM reactor to determine the time response, sensitivity, and selectivity using multiple reagent ions. Of specific importance, we introduced and demonstrated the utility of a dopant-based water vapor suppression system that improves data quality and reduces the number of corrections required during analysis. By comparing detection efficiency for different compounds, we demonstrated that the Vocus AIM captures nearly the entire range of OVOCs, spanning VOCs to ULVOCs, using different types

of reagent ions. Through the optimization of reactor geometry and materials, the time response of the Vocus AIM reactor is greatly improved, even for sticky and reactive compounds. The high sensitivity achieves sub-parts-per-trillion detection limits for a range of VOCs and volatile inorganic compounds (VICs). The innovative design of the new reactor substantially eliminated this humidity sensitivity, facilitating more straightforward measurements of samples with water vapor and simplifying data interpretation. This improvement is crucial for robust and reliable analysis across a spectrum of environmental samples. As a result, the Vocus AIM reactor represents a highly versatile platform able to measure the wide variety of VOCs and VICs in the atmosphere using a single instrument.

Code availability. The gas flow dynamic simulation was performed using the open-source computational fluid dynamics (CFD) software v8 downloaded from http://dl.openfoam.org/ubuntu/dists/focal/main/binary-amd64/ (The OpenFOAM Foundation, 2024) using a customized solver obtained here: https://github.com/pasturm/rhoReactingPimpleFoam (Sturm, 2020).

Data availability. Data are available upon request from the corresponding author.

Supplement. The supplement related to this article is available online at: https://doi.org/10.5194/amt-17-5887-2024-supplement.

Author contributions. MR, VP, and FLH conceptualized the study. MR, VP, CF, PB, SP, SJ, and FLH collected and analyzed the data. PS, UR, and FLH conceptualized the design of the Vocus AIM reactor. MR, VP, and FLH wrote the paper. All authors discussed the results and commented on the paper.

Competing interests. All (co-)authors except Sebastien Perrier and Joel A. Thornton work for Tofwerk AG, which is commercializing the Vocus AIM mass spectrometer.

Disclaimer. Publisher's note: Copernicus Publications remains neutral with regard to jurisdictional claims made in the text, published maps, institutional affiliations, or any other geographical representation in this paper. While Copernicus Publications makes every effort to include appropriate place names, the final responsibility lies with the authors.

Acknowledgements. We would also like to thank Withtech Inc and Minji Park for providing calibration comparison data with the Picarro CRDS.

Review statement. This paper was edited by Keding Lu and reviewed by three anonymous referees.

References

Berndt, T., Richters, S., Kaethner, R., Voigtlander, J., Stratmann, F., Sipila, M., Kulmala, M., and Herrmann, H.: Gas-Phase Ozonolysis of Cycloalkenes: Formation of Highly Oxidized RO_2 Radicals and Their Reactions with NO, NO_2, SO_2, and Other RO_2 Radicals, J. Phys. Chem. A, 119, 10336–10348, https://doi.org/10.1021/acs.jpca.5b07295, 2015.

Berndt, T., Herrmann, H., and Kurten, T.: Direct Probing of Criegee Intermediates from Gas-Phase Ozonolysis Using Chemical Ionization Mass Spectrometry, J. Am. Chem. Soc., 139, 13387–13392, https://doi.org/10.1021/jacs.7b05849, 2017.

Berndt, T., Mentler, B., Scholz, W., Fischer, L., Herrmann, H., Kulmala, M., and Hansel, A.: Accretion Product Formation from Ozonolysis and OH Radical Reaction of alpha-Pinene: Mechanistic Insight and the Influence of Isoprene and Ethylene, Environ. Sci. Technol., 52, 11069–11077, https://doi.org/10.1021/acs.est.8b02210, 2018.

Bertram, T. H., Kimmel, J. R., Crisp, T. A., Ryder, O. S., Yatavelli, R. L. N., Thornton, J. A., Cubison, M. J., Gonin, M., and Worsnop, D. R.: A field-deployable, chemical ionization time-of-flight mass spectrometer, Atmos. Meas. Tech., 4, 1471–1479, https://doi.org/10.5194/amt-4-1471-2011, 2011.

Bianchi, F., Kurten, T., Riva, M., Mohr, C., Rissanen, M. P., Roldin, P., Berndt, T., Crounse, J. D., Wennberg, P. O., Mentel, T. F., Wildt, J., Junninen, H., Jokinen, T., Kulmala, M., Worsnop, D. R., Thornton, J. A., Donahue, N., Kjaergaard, H. G., and Ehn, M.: Highly Oxygenated Organic Molecules (HOM) from Gas-Phase Autoxidation Involving Peroxy Radicals: A Key Contributor to Atmospheric Aerosol, Chem. Rev., 119, 3472–3509, https://doi.org/10.1021/acs.chemrev.8b00395, 2019.

Breitenlechner, M., Fischer, L., Hainer, M., Heinritzi, M., Curtius, J., and Hansel, A.: PTR3: An Instrument for Studying the Lifecycle of Reactive Organic Carbon in the Atmosphere, Anal. Chem., 89, 5824–5831, https://doi.org/10.1021/acs.analchem.6b05110, 2017.

Breitenlechner, M., Novak, G. A., Neuman, J. A., Rollins, A. W., and Veres, P. R.: A versatile vacuum ultraviolet ion source for reduced pressure bipolar chemical ionization mass spectrometry, Atmos. Meas. Tech., 15, 1159–1169, https://doi.org/10.5194/amt-15-1159-2022, 2022.

Bruderer, T., Gaisl, T., Gaugg, M. T., Nowak, N., Streckenbach, B., Müller, S., Moeller, A., Kohler, M., and Zenobi, R.: On-Line Analysis of Exhaled Breath, Chem. Rev., 119, 10803–10828, https://doi.org/10.1021/acs.chemrev.9b00005, 2019.

Caldwell, G. W., Masucci, J. A., and Ikonomou, M. G.: Negative ion chemical ionization mass spectrometry–binding of molecules to bromide and iodide anions, Org. Mass Spectrom., 24, 8–14, https://doi.org/10.1002/oms.1210240103, 1989.

Canaval, E., Hyttinen, N., Schmidbauer, B., Fischer, L., and Hansel, A.: NH_4^+ Association and Proton Transfer Reactions With a Series of Organic Molecules, Front. Chem., 7, 191, https://doi.org/10.3389/fchem.2019.00191, 2019.

Crounse, J. D., Nielsen, L. B., Jørgensen, S., Kjaergaard, H. G., and Wennberg, P. O.: Autoxidation of Organic Com-

pounds in the Atmosphere, J. Phys. Chem. Lett., 4, 3513–3520, https://doi.org/10.1021/jz4019207, 2013.

Donahue, N. M., Epstein, S. A., Pandis, S. N., and Robinson, A. L.: A two-dimensional volatility basis set: 1. organic-aerosol mixing thermodynamics, Atmos. Chem. Phys., 11, 3303–3318, https://doi.org/10.5194/acp-11-3303-2011, 2011.

Dong, F., Li, H., Liu, B., Liu, R., and Hou, K.: Protonated acetone ion chemical ionization time-of-flight mass spectrometry for real-time measurement of atmospheric ammonia, J. Environ. Sci., 14, 66–74, https://doi.org/10.1016/j.jes.2021.07.023, 2022.

Ehn, M., Thornton, J. A., Kleist, E., Sipila, M., Junninen, H., Pullinen, I., Springer, M., Rubach, F., Tillmann, R., Lee, B., Lopez-Hilfiker, F., Andres, S., Acir, I. H., Rissanen, M., Jokinen, T., Schobesberger, S., Kangasluoma, J., Kontkanen, J., Nieminen, T., Kurten, T., Nielsen, L. B., Jorgensen, S., Kjaergaard, H. G., Canagaratna, M., Maso, M. D., Berndt, T., Petaja, T., Wahner, A., Kerminen, V. M., Kulmala, M., Worsnop, D. R., Wildt, J., and Mentel, T. F.: A large source of low-volatility secondary organic aerosol, Nature, 506, 476–479, https://doi.org/10.1038/nature13032, 2014.

Eisele, F. L. and Tanner, D. J.: Measurement of the gas phase concentration of H_2SO_4 and methane sulfonic acid and estimates of H_2SO_4 production and loss in the atmosphere, J. Geophys. Res.-Atmos., 98, 9001–9010, https://doi.org/10.1029/93JD00031, 1993.

Hallquist, M., Wenger, J. C., Baltensperger, U., Rudich, Y., Simpson, D., Claeys, M., Dommen, J., Donahue, N. M., George, C., Goldstein, A. H., Hamilton, J. F., Herrmann, H., Hoffmann, T., Iinuma, Y., Jang, M., Jenkin, M. E., Jimenez, J. L., Kiendler-Scharr, A., Maenhaut, W., McFiggans, G., Mentel, Th. F., Monod, A., Prévôt, A. S. H., Seinfeld, J. H., Surratt, J. D., Szmigielski, R., and Wildt, J.: The formation, properties and impact of secondary organic aerosol: current and emerging issues, Atmos. Chem. Phys., 9, 5155–5236, https://doi.org/10.5194/acp-9-5155-2009, 2009.

Hansel, A., Scholz, W., Mentler, B., Fischer, L., and Berndt, T.: Detection of RO_2 radicals and other products from cyclohexene ozonolysis with NH_4^+ and acetate chemical ionization mass spectrometry, Atmos. Environ., 186, 248–255, https://doi.org/10.1016/j.atmosenv.2018.04.023, 2018.

Isaacman-VanWertz, G., Massoli, P., O'Brien, R., Lim, C., Franklin, J. P., Moss, J. A., Hunter, J. F., Nowak, J. B., Canagaratna, M. R., Misztal, P. K., Arata, C., Roscioli, J. R., Herndon, S. T., Onasch, T. B., Lambe, A. T., Jayne, J. T., Su, L., Knopf, D. A., Goldstein, A. H., Worsnop, D. R., and Kroll, J. H.: Chemical evolution of atmospheric organic carbon over multiple generations of oxidation, Nat. Chem., 10, 462–468, https://doi.org/10.1038/s41557-018-0002-2, 2018.

Ji, Y., Huey, L. G., Tanner, D. J., Lee, Y. R., Veres, P. R., Neuman, J. A., Wang, Y., and Wang, X.: A vacuum ultraviolet ion source (VUV-IS) for iodide–chemical ionization mass spectrometry: a substitute for radioactive ion sources, Atmos. Meas. Tech., 13, 3683–3696, https://doi.org/10.5194/amt-13-3683-2020, 2020.

Kim, M. J., Zoerb, M. C., Campbell, N. R., Zimmermann, K. J., Blomquist, B. W., Huebert, B. J., and Bertram, T. H.: Revisiting benzene cluster cations for the chemical ionization of dimethyl sulfide and select volatile organic compounds, Atmos. Meas. Tech., 9, 1473–1484, https://doi.org/10.5194/amt-9-1473-2016, 2016.

Krechmer, J., Lopez-Hilfiker, F., Koss, A., Hutterli, M., Stoermer, C., Deming, B., Kimmel, J., Warneke, C., Holzinger, R., Jayne, J. T., Worsnop, D. R., Fuhrer, K., Gonin, M., and de Gouw, J. A.: Evaluation of a New Reagent-Ion Source and Focusing Ion-Molecule Reactor for use in Proton-Transfer-Reaction Mass Spectrometry, Anal. Chem., 90, 12011–12018, https://doi.org/10.1021/acs.analchem.8b02641, 2018.

Lavi, A., Vermeuel, M. P., Novak, G. A., and Bertram, T. H.: The sensitivity of benzene cluster cation chemical ionization mass spectrometry to select biogenic terpenes, Atmos. Meas. Tech., 11, 3251–3262, https://doi.org/10.5194/amt-11-3251-2018, 2018.

Lee, B. H., Lopez-Hilfiker, F. D., Mohr, C., Kurten, T., Worsnop, D. R., and Thornton, J. A.: An iodide-adduct high-resolution time-of-flight chemical-ionization mass spectrometer: application to atmospheric inorganic and organic compounds, Environ. Sci. Technol., 48, 6309–6317, https://doi.org/10.1021/es500362a, 2014.

Lee, B. H., Lopez-Hilfiker, F. D., Veres, P. R., McDuffie, E. E., Fibiger, D. L., Sparks, T. M., Ebben, C. J., Green, J. R., Schroder, J. C., Campuzano-Jost, P., Iyer, S., D'Ambro, E. A., Schobesberger, S., Brown, S. S., Wooldridge, P. J., Cohen, R. C., Fiddler, M. N., Bililign, S., Jimenez, J. L., Kurtén, T., Weinheimer, A. J., Jaegle, L., and Thornton, J. A.: Flight Deployment of a High-Resolution Time-of-Flight Chemical Ionization Mass Spectrometer: Observations of Reactive Halogen and Nitrogen Oxide Species, J. Geophys. Res.-Atmos., 123, 7670–7686, https://doi.org/10.1029/2017JD028082, 2018.

Li, Y., Pöschl, U., and Shiraiwa, M.: Molecular corridors and parameterizations of volatility in the chemical evolution of organic aerosols, Atmos. Chem. Phys., 16, 3327–3344, https://doi.org/10.5194/acp-16-3327-2016, 2016.

Li, D., Wang, D., Caudillo, L., Scholz, W., Wang, M., Tomaz, S., Marie, G., Surdu, M., Eccli, E., Gong, X., Gonzalez-Carracedo, L., Granzin, M., Pfeifer, J., Rörup, B., Schulze, B., Rantala, P., Perrier, S., Hansel, A., Curtius, J., Kirkby, J., Donahue, N. M., George, C., El-Haddad, I., and Riva, M.: Ammonium CI-Orbitrap: a tool for characterizing the reactivity of oxygenated organic molecules, Atmos. Meas. Tech. Discuss. [preprint], https://doi.org/10.5194/amt-2023-149, in review, 2023.

Lopez-Hilfiker, F. D., Iyer, S., Mohr, C., Lee, B. H., D'Ambro, E. L., Kurtén, T., and Thornton, J. A.: Constraining the sensitivity of iodide adduct chemical ionization mass spectrometry to multifunctional organic molecules using the collision limit and thermodynamic stability of iodide ion adducts, Atmos. Meas. Tech., 9, 1505–1512, https://doi.org/10.5194/amt-9-1505-2016, 2016.

Mazzucotelli, M., Farneti, B., Khomenko, I., Gonzalez-Estanol, K., Pedrotti, M., Fragasso, M., Capozzi, V., and Biasioli, F.: Proton transfer reaction mass spectrometry: A green alternative for food volatilome profiling, Green Analytical Chemistry, 3, 100041, https://doi.org/10.1016/j.greeac.2022.100041, 2022.

Morris, M. A., Pagonis, D., Day, D. A., de Gouw, J. A., Ziemann, P. J., and Jimenez, J. L.: Absorption of volatile organic compounds (VOCs) by polymer tubing: implications for indoor air and use as a simple gas-phase volatility separation technique, Atmos. Meas. Tech., 17, 1545–1559, https://doi.org/10.5194/amt-17-1545-2024, 2024.

Palm, B. B., Liu, X., Jimenez, J. L., and Thornton, J. A.: Performance of a new coaxial ion–molecule reaction region for low-

pressure chemical ionization mass spectrometry with reduced instrument wall interactions, Atmos. Meas. Tech., 12, 5829–5844, https://doi.org/10.5194/amt-12-5829-2019, 2019

Pfeifer, J., Simon, M., Heinritzi, M., Piel, F., Weitz, L., Wang, D., Granzin, M., Müller, T., Bräkling, S., Kirkby, J., Curtius, J., and Kürten, A.: Measurement of ammonia, amines and iodine compounds using protonated water cluster chemical ionization mass spectrometry, Atmos. Meas. Tech., 13, 2501–2522, https://doi.org/10.5194/amt-13-2501-2020, 2020.

Reinecke, T., Leiminger, M., Jordan, A., Wisthaler, A., and Müller, M.: Ultrahigh Sensitivity PTR-MS Instrument with a Well-Defined Ion Chemistry, Anal. Chem., 95, 11879–11884, https://doi.org/10.1021/acs.analchem.3c02669, 2023.

Rissanen, M. P., Mikkilä, J., Iyer, S., and Hakala, J.: Multi-scheme chemical ionization inlet (MION) for fast switching of reagent ion chemistry in atmospheric pressure chemical ionization mass spectrometry (CIMS) applications, Atmos. Meas. Tech., 12, 6635–6646, https://doi.org/10.5194/amt-12-6635-2019, 2019.

Riva, M., Rantala, P., Krechmer, J. E., Peräkylä, O., Zhang, Y., Heikkinen, L., Garmash, O., Yan, C., Kulmala, M., Worsnop, D., and Ehn, M.: Evaluating the performance of five different chemical ionization techniques for detecting gaseous oxygenated organic species, Atmos. Meas. Tech., 12, 2403–2421, https://doi.org/10.5194/amt-12-2403-2019, 2019.

Schobesberger, S., D'Ambro, E. L., Vettikkat, L., Lee, B. H., Peng, Q., Bell, D. M., Shilling, J. E., Shrivastava, M., Pekour, M., Fast, J., and Thornton, J. A.: Airborne flux measurements of ammonia over the southern Great Plains using chemical ionization mass spectrometry, Atmos. Meas. Tech., 16, 247–271, https://doi.org/10.5194/amt-16-247-2023, 2023.

Sturm, P.: rhoReactingPimpleFoam, GitHub [code], https://github.com/pasturm/rhoReactingPimpleFoam (last access: 13 September 2024), 2020.

Tang, J., Schurgers, G., and Rinnan, R.: Process Understanding of Soil BVOC Fluxes in Natural Ecosystems: A Review, Rev. Geophys., 57, 966–986, https://doi.org/10.1029/2018RG000634, 2019.

The OpenFOAM Foundation: OpenFOAM Binary/Source Package Repository, http://dl.openfoam.org/ubuntu/dists/focal/main/binary-amd64/, last access: 13 September 2024.

Vasquez, K. T., Allen, H. M., Crounse, J. D., Praske, E., Xu, L., Noelscher, A. C., and Wennberg, P. O.: Low-pressure gas chromatography with chemical ionization mass spectrometry for quantification of multifunctional organic compounds in the atmosphere, Atmos. Meas. Tech., 11, 6815–6832, https://doi.org/10.5194/amt-11-6815-2018, 2018.

Xu, L., Coggon, M. M., Stockwell, C. E., Gilman, J. B., Robinson, M. A., Breitenlechner, M., Lamplugh, A., Crounse, J. D., Wennberg, P. O., Neuman, J. A., Novak, G. A., Veres, P. R., Brown, S. S., and Warneke, C.: Chemical ionization mass spectrometry utilizing ammonium ions (NH_4^+ CIMS) for measurements of organic compounds in the atmosphere, Atmos. Meas. Tech., 15, 7353–7373, https://doi.org/10.5194/amt-15-7353-2022, 2022.

Ye, C., Yuan, B., Lin, Y., Wang, Z., Hu, W., Li, T., Chen, W., Wu, C., Wang, C., Huang, S., Qi, J., Wang, B., Wang, C., Song, W., Wang, X., Zheng, E., Krechmer, J. E., Ye, P., Zhang, Z., Wang, X., Worsnop, D. R., and Shao, M.: Chemical characterization of oxygenated organic compounds in the gas phase and particle phase using iodide CIMS with FIGAERO in urban air, Atmos. Chem. Phys., 21, 8455–8478, https://doi.org/10.5194/acp-21-8455-2021, 2021.

Yuan, B., Koss, A. R., Warneke, C., Coggon, M., Sekimoto, K., and de Gouw, J. A.: Proton-Transfer-Reaction Mass Spectrometry: Applications in Atmospheric Sciences, Chem. Rev., 117, 13187–13229, https://doi.org/10.1021/acs.chemrev.7b00325, 2017.

You, Y., Kanawade, V. P., de Gouw, J. A., Guenther, A. B., Madronich, S., Sierra-Hernández, M. R., Lawler, M., Smith, J. N., Takahama, S., Ruggeri, G., Koss, A., Olson, K., Baumann, K., Weber, R. J., Nenes, A., Guo, H., Edgerton, E. S., Porcelli, L., Brune, W. H., Goldstein, A. H., and Lee, S.-H.: Atmospheric amines and ammonia measured with a chemical ionization mass spectrometer (CIMS), Atmos. Chem. Phys., 14, 12181–12194, https://doi.org/10.5194/acp-14-12181-2014, 2014.

Zhang, W., Xu, L., and Zhang, H.: Recent advances in mass spectrometry techniques for atmospheric chemistry research on molecular-level, Mass Spectrom. Rev., 43, 1091–1134, https://doi.org/10.1002/mas.21857, 2023.

Zhang, Y., Liu, R., Yang, D., Guo, Y., Li, M., and Hou, K.: Chemical ionization mass spectrometry: Developments and applications for on-line characterization of atmospheric aerosols and trace gases, TrAC-Trend. Anal. Chem., 168, 117353, https://doi.org/10.1016/j.trac.2023.117353, 2023.